

## Anomalous pulse delay in microwave propagation: A plausible connection to the tunneling time

A. Ranfagni, P. Fabeni, G.P. Pazzi, and D. Mugnai

*Istituto di Ricerca sulle Onde Elettromagnetiche, del Consiglio Nazionale delle Ricerche, Via Panciatichi 64, 50127 Firenze, Italy*

(Received 17 February 1993)

Measures of pulse delay in microwave propagation, in open air and for short distances (not much greater than 1 m), were made by using launcher and receiver horns. When these are facing each other we observe a delay time corresponding to a speed equal to  $c$  while, if the receiver horn is shifted or tilted with respect to the launcher horn, the delay time decreases showing a superluminal behavior. In other words the modulation phase shift, interpreted as a propagation time, turns out to be surprisingly smaller than the one relative to the light speed. This effect, which disappears for longer distances, is here interpreted on the basis of the existence of a special kind of evanescent waves (leaky waves). Just the presence of evanescent waves allows one to make a comparison with the tunneling processes where superluminal transport properties have been theoretically predicted.

PACS number(s): 03.40.Kf, 73.40.Gk

### I. INTRODUCTION

The problem of the tunneling time has not yet received a definite explanation in spite of many efforts performed thus far. The question is whether there exists a physical quantity, with dimension of time, which characterizes the particle motion through the barrier. The general belief is that there is not a fairly clear definition of such a quantity: the several proposals run from pure semiclassical to fully quantum mechanical models including or not relativistic effects [1].

One remarkable feature of barrier penetration in quantum theory is that a particle traversing a barrier appears to do so in zero time but an actual check of this effect is reputed impossible [2]. There are in fact considerable difficulties in performing a direct experimental test mainly because of the very short times involved and of the complexity of these kinds of experiments [3].

These complications can be partially surmounted with a microwave setup where a sub-cutoff waveguide simulates a quantum-mechanical potential barrier. This allows us to make experiments in a very accessible temporal range and to compare the results with several models, suitably translated into the electromagnetic framework [4]. The analogy between particle motion and electromagnetic wave propagation is based on the similarity of the dispersion relation and on a close correspondence of the wave equation, especially when relativistic expressions are considered [5]. However, contrary to the particle case where the measure of the arrival time is a quantum-mechanical disturbing procedure, an electromagnetic pulse can consist of many photons and can be probed in a noninvasive way [6].

In this manner it was possible to establish that among the several models, the phase time one, already proposed by Hartman [7], appears the most appropriate for de-

scribing the experimental results of pulse delay in a relatively large range of parameter values (frequency, barrier length). However, it was not possible to investigate sufficiently below the cutoff frequency for the severe limitations due to the attenuation of the signal [8].

Recently [9] an extension of the measurements sensibly below the cutoff has been achieved by a Fourier-transform technique—based on the superposition principle of the linear Maxwell equations—applied to the same microwave setup of Ref. [4]. The obtained results confirm the validity of the phase-time model [6,7] according to which the delay is given by

$$\tau_{\phi} = \frac{\Delta\phi}{\Delta\omega}, \quad (1)$$

where  $\Delta\omega$  is the frequency variation and  $\Delta\phi$  the phase change which depends only on the boundary conditions at the ends of the sub-cutoff section of the waveguide and is independent of its length. This implies that for sufficiently long length—say 10 cm for a cutoff around 10 GHz—the tunneling in the barrier turns out to be a superluminal motion. More precisely, since there is no phase variation of the wave inside the barrier (evanescent wave), the pulse transit through the barrier itself seems to be instantaneous—a direct consequence of the results of Ref. 9—perhaps “not in any clear sense a paradox” [6], nevertheless, an interesting result.

Superluminal transport properties for electromagnetic modes have been also predicted in some theoretical works on optical tunneling [10]. Dealing with the microwave simulation of tunneling, a theoretical interpretation was modeled on the basis of a path-integral solution of the telegrapher’s equation, analytically continued to imaginary time [11]. There, it was shown that in tunneling processes the effective (imaginary) velocity turns out to

be increased by dissipative effects and can actually overcome the light velocity  $c$ , contrary to the classically allowed motion where the effective velocity has  $c$  as upper bound ([Eqs. (9) and (10) in Ref. 11]).

The fact that the tunneling motion can become superluminal creates a controversial question [12], which deserves a deeper understanding and, to this purpose, we have extended the investigation with microwaves. However, due to the difficulties of signal attenuation sufficiently below the cutoff with evanescent waves inside the guide, we have tested evanescent waves in an “open-air” transmission experiment. In such a way we can easily measure the delay time of a pulse-modulated carrier and deduce information about the signal velocity connected with evanescent modes in strict analogy with tunneling.

In Sec. II we briefly describe such a microwave experiment. The relative results of pulse delay are then analyzed in Sec. III and discussed, in connection to tunneling, in Sec. IV. Some analytical details are reported in the Appendix.

## II. PULSE-DELAY MEASUREMENTS

The appearance of a paper [13] dealing with microwaves which travel faster than the speed of light over a distance of about  $\frac{1}{2}$  m, in a waveguide and open air, attracted our interest and we decided to repeat the experiments. The  $X$ -band microwave setup is basically the same as our previous measurements of delay time in a narrowed waveguide [4]. A microwave signal like a step function is supplied by a klystron (at a frequency  $\nu_0 \approx 9.5$  GHz) modulated by a pin modulator, whose fall time (less than 10 ns) is suitable to measure delay times down to less than 1 ns. First, the signals taken at two selected points in the  $X$ -band circuit are sent to a high temporal resolution oscilloscope (Tektronix 2440) able to measure the delay with an accuracy of  $\sim 0.1$  ns. As known, the phase velocity  $v_p$  and the group velocity  $v_g$ , for a  $TE_{01}$  mode in a rectangular waveguide, are given by [14]

$$\frac{c}{v_p} = \frac{v_g}{c} = \sqrt{1 - \left(\frac{\lambda}{2b}\right)^2}, \quad (2)$$

where  $\lambda$  is the free-space wavelength and  $b$  is the width of the guide. Although the phase velocity is greater than  $c$ , the signal propagates according to the group velocity which for propagating waves, that is for  $\lambda < 2b$ , is always less than  $c$ . As a test of the apparatus we report in Table I the results relative to  $L = 90$  cm of waveguide in the  $X$  band ( $b = 22.86$  mm), free-space delay  $L/c = 3$  ns, which confirms a well-known behavior and not that of Ref. [13], which reports signal velocity data in agreement with the

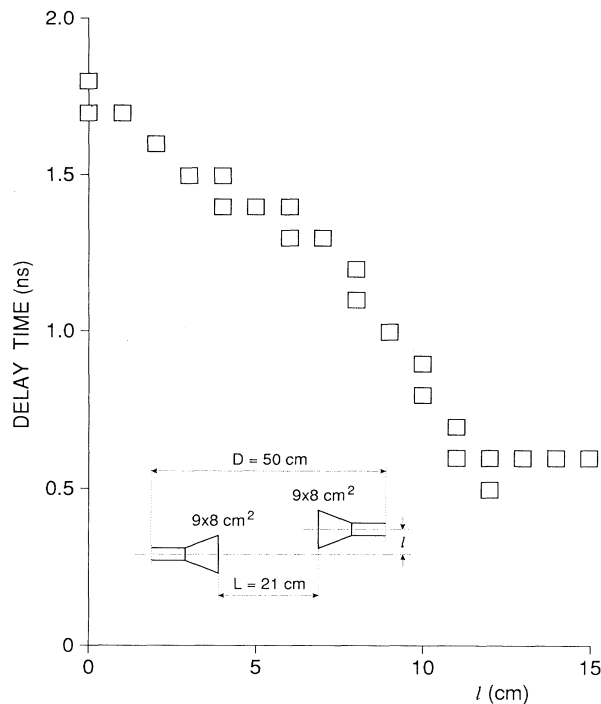


FIG. 1. Pulse delay in the transmission at 9.5 GHz as a function of the perpendicular displacement  $l$  (in the  $H$  plane) of the receiver horn while the length  $L = 21$  cm is taken as a constant. The distance  $D = 50$  cm represents the separation between the two detectors: when they are directly connected by a waveguide of the same length, the delay is 2.2 ns. When the waveguide is substituted by the two horns (flare angle of  $50^\circ$ ) facing each other and separated by 21 cm, the delay decreases to 1.7–1.8 ns, as expected.

phase velocity in the waveguide.

Successively, in the open-air experiment, we employ launcher and receiver pyramidal horns facing each other and separated by a distance of the order of tens of centimeters and we measure the pulse delay obtaining a propagating speed equal to  $c$ , as expected. Then the receiver horn is shifted transversely (Figs. 1–5) or the launcher is tilted (Figs. 6 and 7). In both cases we observe a shortening of the delay time while the distance is certainly not decreased, now in agreement with the results of Ref. [13]. This effect, observed over distances from  $\sim 10$  cm to  $\sim 100$  cm, is more pronounced at lower distances and is present either by varying the geometry in the  $H$  plane or in the  $E$  plane. For greater distances

TABLE I. Comparison at two frequencies of the evaluated and measured pulse delay relative to a waveguide in  $X$  band, mode  $TE_{01}$ , with a length  $L = 90$  cm.

$\nu_0$ (GHz)	$\lambda = c/\nu_0$ (cm)	$v_p/c$	$v_g/c$	$\tau = L/v_g$ (ns)	$\tau_{\text{measur.}}$ (ns)
9	3.333	1.461	0.684	4.383	$4.3 \pm 0.1$
9.5	3.158	1.383	0.723	4.149	$4.1 \pm 0.1$

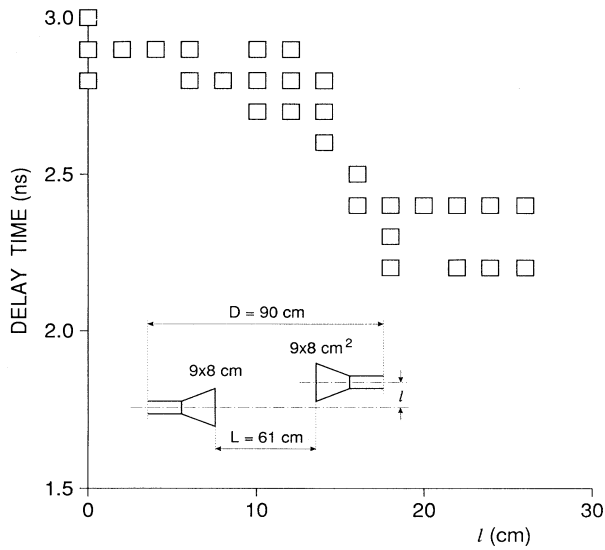


FIG. 2. Same as Fig. 1 with  $D = 90$  cm and  $L = 61$  cm.

the effect becomes unobservable.

In Figs. 1–3 we report the results of delay time obtained with two identical horn antennas ( $9 \times 8$  cm<sup>2</sup> of aperture) separated by a different length  $L$  as a function of the perpendicular displacement  $l$ . We note that the shortening of the delay time is more evident for the shorter distance ( $L = 21$  cm), it is still present for the intermediate one ( $L = 61$  cm), while it is practically absent at the longer one ( $L = 111$  cm). In Figs. 4 and 5 we report the results obtained with a launcher consisting of a horn of a greater aperture ( $13.5 \times 10.5$  cm<sup>2</sup>) for two distances,  $L = 49$  cm and  $L = 99$  cm, and we observe an analogous, more evident, effect. By considering the involved quantities, it clearly emerges to be a superluminal behavior especially at lower distances.

Results of delay time obtained as a function of the tilting angle  $\alpha$  of the launcher are shown in Figs. 6 and 7. Here we report directly the ratio  $\tau(\alpha = 0)/\tau(\alpha)$  so that the points represent the signal velocity ( $v_s$ ) relative to

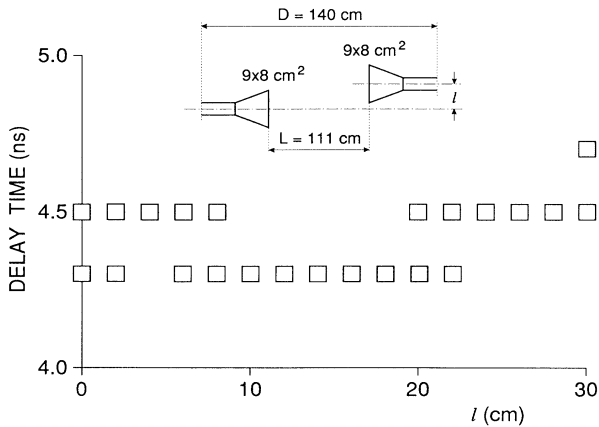


FIG. 3. Same as Fig. 1 with  $D = 140$  cm and  $L = 111$  cm.

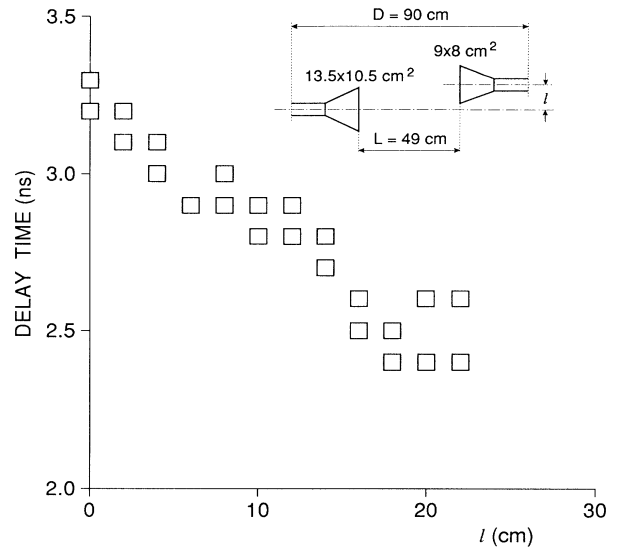


FIG. 4. Same as Fig. 1 with the launcher of a greater aperture (flare angle of  $40^\circ$ ),  $D = 90$  cm and  $L = 49$  cm.

the velocity for  $\alpha = 0$ , which we assume to be coincident with the light velocity [15]. We note that the ratio  $v_s/c$  strongly increases by increasing the tilting angle  $\alpha$ .

### III. DELAY-TIME ANALYSIS

In this section we shall try to explain the “anomalous” pulse-delay results reported in Sec. II. First we wish to note that we are not dealing with normal long-range propagation but rather with some local effect whose understanding would require analysis of the near field. This suggests that we are concerned with evanescent waves whose importance, with respect to the “normal” contribution, tends to disappear sufficiently far from the launcher.

Let us assume that the radiated field from the launcher can be expressed as that of a rectangular aperture having the dimensions of the mouth of the horn launcher.

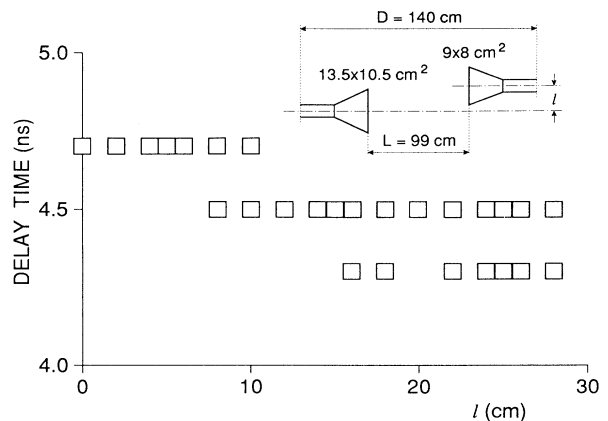


FIG. 5. Same as Fig. 4 with  $D = 140$  cm and  $L = 99$  cm.

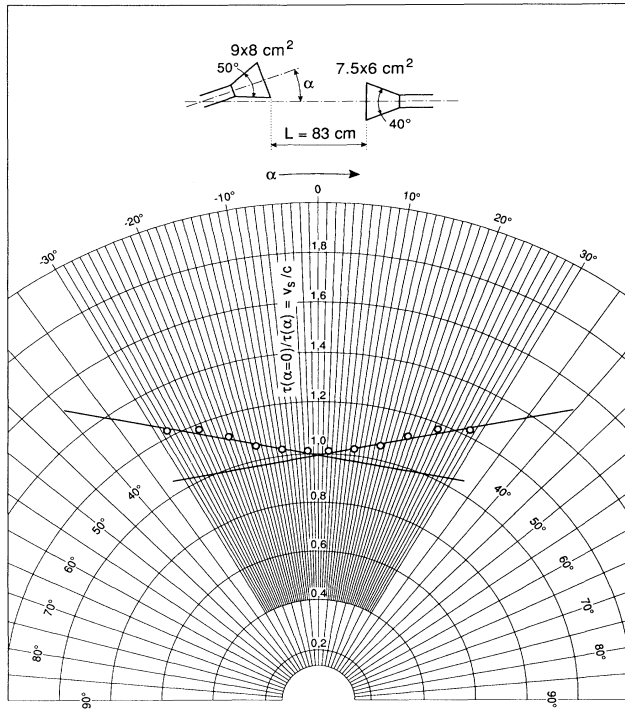


FIG. 6. Ratio of the pulse delay at 9.5 GHz for  $\alpha = 0$  to that for the  $\alpha$  variable, or signal velocity normalized to the light speed, as a function of the tilting angle  $\alpha$  for a separation  $L = 83$  cm between the two horns whose dimensions are given in the inset. The experimental points are fitted by the straight lines represented by Eq. (8) with  $\beta_r = \pm 11^\circ$  and  $\beta_i = 11.5^\circ$ .

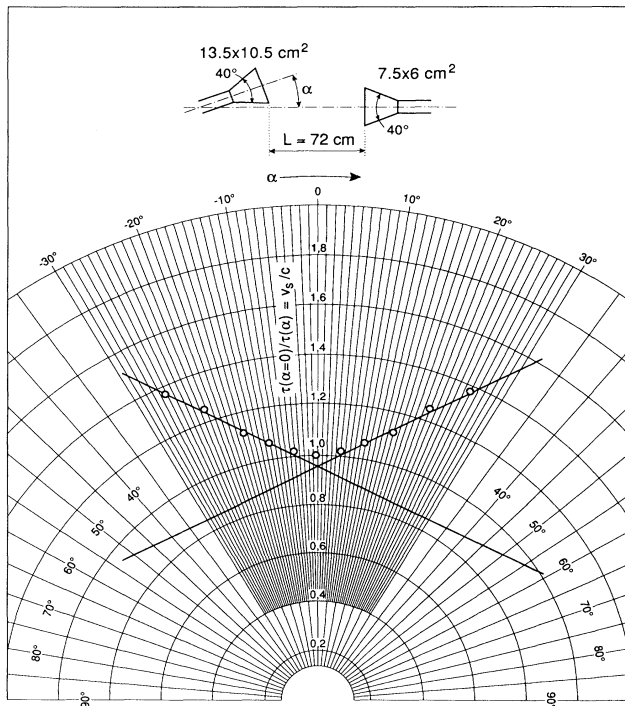


FIG. 7. Same as Fig. 6 with the launcher of a greater aperture and  $L = 72$  cm. The experimental points are fitted by the straight lines represented by Eq. (8) with  $\beta_r = \pm 27^\circ$  and  $\beta_i = 33.5^\circ$ .

For simplicity's sake let us also consider the aperture as infinite along  $\zeta$ ; that is, we assume the phenomenon to be independent of this coordinate,  $\xi$ ,  $\eta$ , and  $\zeta$  being the reference axes whose origin  $O$  is put in the center of the aperture (see Fig. 8). Under these assumptions the total beam in the semispace  $\xi > 0$  can be expressed, in the scalar approximation, as a superposition of plane waves in the form [16],

$$F(\xi, \eta) = e^{-i\omega t} \int_{-\pi/2}^{\pi/2} A(z) \exp[ik(\xi \cos z + \eta \sin z)] dz, \quad (3)$$

where  $z$  is the angle of the normal of the elementary wave [whose amplitude is  $A(z)$ ] with the  $\xi$  axis,  $k = 2\pi/\lambda$  is the wave number, and  $\omega = 2\pi\nu$  is the angular frequency. As known, in order to reproduce the field distribution in the plane  $\Sigma$  of the aperture, we have to extend the limits of integration of the  $z$  angle in the complex plane. By putting

$$z = x + iy$$

and

$$\xi = \rho \cos \alpha, \quad \eta = \rho \sin \alpha,$$

where  $\rho$  and  $\alpha$  are the polar coordinates of the observation point  $P$ , the integral in Eq. (3) becomes

$$\int_C A(z) \exp[ik\rho \cos(z - \alpha)] dz, \quad (4)$$

where the integration path  $C$  is represented in Fig. 9. For  $\rho \gg \lambda$  we can evaluate the integral (4) asymptotically by the saddle-point method. In such a way the integration path is deformed into the steepest-descent path  $C'$  (see Fig. 9) which is given by one branch of the transcendental equation [17]

$$\cos(x - \alpha) \cosh y = 1, \quad (5)$$

which crosses the real axis at  $z = \alpha$  with an angle equal to  $-\pi/4$ . In deforming the path we have to consider the pole contribution if the amplitude  $A(z)$  contains a singularity

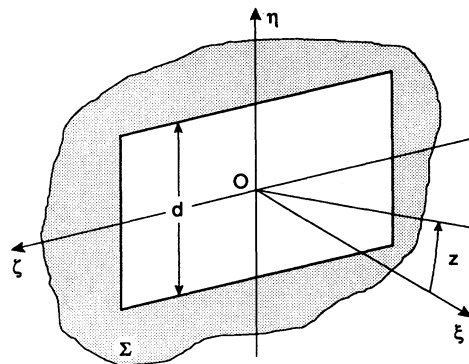


FIG. 8. Schematic of the mouth of the horn launcher as an aperture in the  $\Sigma$  plane with the adopted coordinate axes.

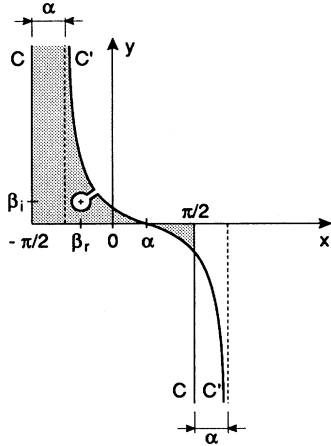


FIG. 9. The original integration path  $C$  of Eq. (4) is deformed into the steepest descent path  $C'$  taking into account the presence of the pole singularities. If these are situated into the shaded areas the corresponding leaky waves have phase-path velocity greater than  $c$ .

in the region of deformation of the path. Let us suppose that there is a pole at the complex point  $\beta = \beta_r + i\beta_i$  (this assumption will be justified in the Appendix). In this case the integral (4) can be expressed as

$$\sqrt{\frac{\lambda}{\rho}} e^{i(k\rho - \frac{\pi}{4})} A(\alpha) + 2\pi i \operatorname{res}[A(z \rightarrow \beta)] e^{ik\rho \cos(\beta - \alpha)}, \quad (6)$$

where the first term represents the normal contribution (a cylindrical wave) and the second, due to the pole, an evanescent wave. By putting  $\operatorname{res}[A(z \rightarrow \beta)] = \bar{A}(\beta)$  and remembering that  $\beta = \beta_r + i\beta_i$ , the contribution due to the pole can be written as

$$2\pi i \bar{A}(\beta) \exp[ik\rho \cos(\beta_r - \alpha) \cosh \beta_i + k\rho \sin(\beta_r - \alpha) \sinh \beta_i]. \quad (7)$$

This represents a wave propagating in the  $\beta_r$  direction whose amplitude attenuates with increasing  $\alpha$  and  $\rho$ , as sketched in Fig. 10, while for  $\beta_r \rightarrow \alpha$  (if  $\beta_i \rightarrow 0$ ), its contribution may be the dominant one in (6).

These kinds of waves, which do not exist for  $\alpha$  sufficiently large (for  $\beta_r \sim \beta_i$  this happens for  $\alpha \sim 0$ , see Fig. 9) are named *leaky waves* [16,17]. As for the phase factor we note that, recovering also the time dependence, it exhibits a propagation velocity along a path with an angle  $\alpha$  (phase-path velocity)

$$v_{PP} \equiv \frac{\omega}{k'} = \frac{\omega}{k} \frac{1}{\cos(\beta_r - \alpha) \cosh \beta_i} = \frac{c}{\cos(\beta_r - \alpha) \cosh \beta_i} \quad (8)$$

which, depending on the position of the pole  $\beta$  and on the observation angle  $\alpha$ , can be greater or smaller than the light velocity  $c$ , the border line being given by Eq. (5). We wish to note that in a nondispersive situation, like that of our experiment (open-air propagation), rela-

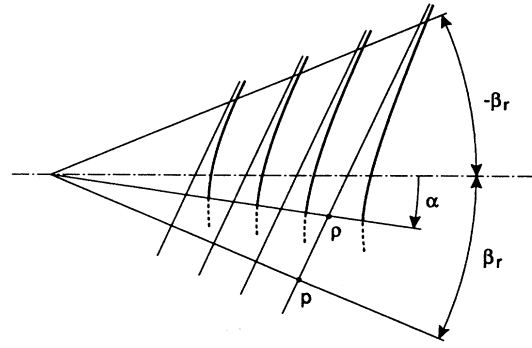


FIG. 10. The existence domain of the leaky waves (whose amplitudes are sketched along the phase front) is practically confined to angle values  $\alpha$  such that  $-\beta_r \leq \alpha \leq \beta_r$ , if  $\beta_i \sim 0$ . With increasing  $\beta_i$  this domain is reduced in the higher-amplitude side, for  $\beta_i \sim \beta_r$  this happens around  $\alpha = 0$ .

tion (8) can be assumed to hold also for the signal path velocity. In these conditions, since  $(\Delta\omega/\Delta k) = (\omega/k)$ , Eq. (1) simply becomes

$$\tau_\phi = \frac{L}{v_{PP}} = \frac{Lk'(\alpha, \beta)}{\omega} = \frac{\phi'(\alpha, \beta)}{\omega}. \quad (9)$$

In this way we can obtain, for  $\alpha < \beta_r$ , signal velocities apparently greater than  $c$  [18]. The results of signal velocity reported in Figs. 6 and 7 can be interpreted according to Eq. (8), which holds for both sides of the angle  $\alpha$ , as indicated by the straight lines which well fit the experimental data with plausible values of  $\beta_r$  and  $\beta_i$ . We note that the values of  $\beta_r$  are roughly comparable with one half of the flare angle of the horn; that is, the leaky waves appear to be in some way related to the vertical walls of the launcher (in fact by using biconical horns, vertically polarized, this “anomalous” effect is no longer observable in the  $H$  plane). In addition, the values of  $\beta_i$  comparable with  $\beta_r$  ones make the leaky waves observable only for negative  $\alpha$  values, as expected.

#### IV. RELEVANCE OF THE RESULTS TO THE TUNNELING

The “anomalous” pulse delay reported in Sec. II and analyzed in Sec. III can be considered as experimental evidence about the existence of a special kind of evanescent waves—the leaky waves—in the near field radiated by horn antennas. Our interest lies particularly in the delay-time behavior of a modulated carrier, intended as an indicator of the signal velocity in the presence of evanescent waves.

It turns out that the delay of the signal sensibly decreases when the observation angle  $\alpha$  is appreciably different from  $\beta_r$ ; that is, the considered path is inclined with respect to the direction of  $\beta_r$ . The angle  $\alpha$  cannot be augmented much beyond the opposite side ( $-\beta_r$ ); that is, the maximum of the path slope is approximately comparable with the flare angle of the launcher, where we observe an increase of the signal velocity of the order

of 40%. Nevertheless we can argue that the trend is certainly that of obtaining zero delay for paths tending to be coincident with the wave front. In this limit, that is for  $(\beta_r - \alpha) \rightarrow \pi/2$ , Eq. (7) exactly gives infinite velocity, hence zero delay [2]. This picture appears almost analogous to the tunneling one as realized by the microwave simulation with a sub-cutoff waveguide where evanescent waves are operating [4].

The only difference is that, in the case of a waveguide, dispersion is present. This fact makes the analysis of the signal shape more complicated, for the spreading of the wave packet, especially in a tunneling situation where the forerunners strongly influence the time of arrival of the signal [19]. However, in a typical situation this is not considered too severe a limitation such that without considering this effect the results are not significant [10]. We wish to recall that in both cases—with or without dispersion—the upper limit of the signal velocity, in classically allowed motions, is represented by the light speed as demonstrated for wave propagation in dispersive media in Ref. [20], and in electric lines in Ref. [21]. However, such arguments do not appear clearly applicable to classically forbidden processes or evanescent waves.

It seems therefore quite plausible that in tunneling there are superluminal motions as evidenced in Ref. [9], implicitly admitted also in Ref. [11], and supported by the results here presented. A promising tool for a further theoretical investigation of this problem still appears to be the application of the telegrapher's equation, as outlined in Ref. [11], according to the developments of Ref. [22]. In particular, we intend to investigate the properties of the distribution function of the randomized time as it results from the superposition of “undisturbed” normal processes and “disturbed” ones, which in tunneling situations behave as accelerated processes.

Noteworthy is also the fact that tunneling time could be considered a practical case of a *weak value* observable in the framework of the *weak measurement* theory [23]. In this case mean values, which would be strictly forbidden for any complete ensemble, can be obtained for a subensemble.

*Note added.* After this work was completed, we received a copy of an unpublished work by A.M. Steinberg, P.G. Kwiat, and R.Y. Chiao dealing with measurements of single-photon tunneling time. They also find an apparent superluminal tunneling velocity but they do not repute it as a genuine signal velocity, rather a case of weak-value observable [23].

#### ACKNOWLEDGMENTS

We enjoyed discussions with Laura Ronchi Abbozzo and Marco Bini: the latter notified us of the work by T. Koryu Ishii and G.C. Giakos [13]. Thanks are due to Amleto Ignesti and Carlo Bacci for technical assistance.

#### APPENDIX: ESTIMATE OF THE AMPLITUDE FUNCTION

The analysis of the leaky waves of Sec. III is based on the assumption that the amplitude function  $A(z)$  in the

integral of Eq. (3) contains a pole singularity at a complex point  $\beta$  in the  $z$  plane. This assumption can be justified by analyzing the radiated field in a quasi-near-field approximation, that is by abandoning the Fraunhofer approach and adopting something like the Huygens-Fresnel one [24].

The geometry of our experiment, with a distance of observation  $\rho \approx 1/2$  m, wavelength  $\lambda \approx 3$  cm, and dimension of the aperture of the launcher  $d \approx 10$  cm, is just intermediate between a far-field and a near-field situation; therefore, we shall try to model a suitable approach.

Let us consider the aperture in the  $\Sigma$  plane of Fig. 8 as divided into a number ( $2N$ ) of horizontal zones (width  $d/2N$ ) as sketched in Fig. 11. The field in a point  $P(\xi, \eta)$  can be expressed by writing  $F(\xi, \eta)$  in Eq. (3)—we omit the time dependence—as

$$F(\xi, \eta) = \int A(z) e^{ik(\xi \cos z + \eta \sin z)} dz \\ = \sum_n \int A(z_n) e^{ik(\xi \cos z_n + \eta \sin z_n)} dz_n, \quad (\text{A1})$$

where the integer index  $n$  runs from  $-N$  to  $N$  and the amplitude  $A(z_n)$ , relative to the  $n$ th zone, is given by

$$A(z_n) = \int_{-\infty}^{\infty} F(\eta_n) e^{-ik\eta_n \sin z_n} d\eta_n. \quad (\text{A2})$$

Here  $F(\eta_n)$  is the field intensity, in the  $\Sigma$  plane, assumed as constant across the considered zone and zero elsewhere. By substituting (A2) into (A1) we have

$$F(\xi, \eta) = \sum_n \int \left( \int F(\eta_n) e^{-ik\eta_n \sin z_n} d\eta_n \right) \\ \times e^{ik(\xi \cos z_n + \eta \sin z_n)} dz_n. \quad (\text{A3})$$

An approximation usually made for evaluating (A3) consists in inverting the order of integrations (before  $\int dz_n$  and then  $\int d\eta_n$ ) and to factorize  $\sin z_n$ , namely [24]

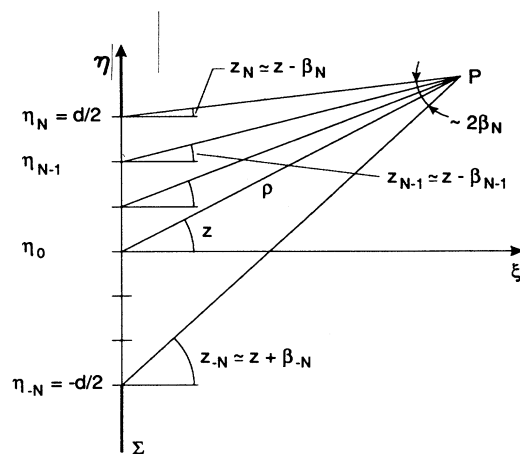


FIG. 11. The aperture (width  $d$ ) in the  $\Sigma$  plane is divided into  $2N$  zones and the field in the point  $P$  is evaluated as a superposition of the several contributions.

$$F(\xi, \eta) = \sum_n \int F(\eta_n) d\eta_n \int e^{ik[\xi \cos z_n + (\eta - \eta_n) \sin z_n]} dz_n, \quad (\text{A4})$$

and inverting  $\sum_n$  with  $\int d\eta_n$ , we assume  $F(\eta_n) \equiv F(\eta)$ ,

$$F(\xi, \eta) = \int F(\eta) d\eta \sum_n \int e^{ik[\xi \cos z_n + (\eta - \eta_n) \sin z_n]} dz_n. \quad (\text{A5})$$

We proceed conversely by factorizing  $\int dz_n$  in order to recover a form like Eq. (A3): this procedure is acceptable by considering that we are studying the field at relatively large distances,  $\rho > d > \lambda$ . So we obtain the approximate result

$$\begin{aligned} F(\xi, \eta) &= \int A(z) e^{ik(\xi \cos z + \eta \sin z)} dz \\ &\approx \int \left( \sum_n \int F(\eta_n) e^{-ik\eta_n \sin z_n} d\eta_n \right) \\ &\quad \times e^{ik(\xi \cos z + \eta \sin z)} dz, \end{aligned} \quad (\text{A6})$$

where the amplitude  $A(z)$  has become

$$A(z) = \sum_n \int F(\eta_n) e^{-ik\eta_n \sin z_n} d\eta_n. \quad (\text{A7})$$

Assuming for simplicity  $F(\eta_n) \equiv F(\eta) = \text{const}$ , the integration in (A7) is immediate and we obtain for  $A(z)$ , or more exactly  $A(\sin z)$ ,

$$\begin{aligned} A(\sin z) &= \sum_n \frac{\cos z}{2\pi} \int_{\eta_{n-1}}^{\eta_n} e^{-ik\eta \sin z} d\eta \\ &= \sum_n \frac{\cos z}{2\pi} \left[ \frac{e^{-ik\eta \sin z}}{-ik \sin z} \right]_{\eta_{n-1}}^{\eta_n}. \end{aligned} \quad (\text{A8})$$

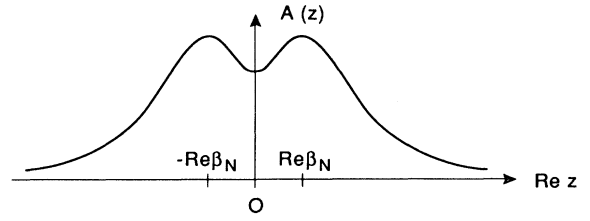


FIG. 12. Field intensity in the proximity of the aperture. The two peaks correspond to  $\pm\beta_N$  [Eq. (A9)].

By expressing the angle  $z_n = z - \beta_n$  and performing the summation (crucial is the variation of the angle  $z_n$  as a function of  $\eta$ , see Fig. 11) we get the approximate result

$$A(\sin z) = \frac{\cos z}{2\pi} \left[ \frac{e^{-ik \frac{d}{2} \sin(z - \beta_N)}}{-ik \sin(z - \beta_N)} - \frac{e^{ik \frac{d}{2} \sin(z + \beta_N)}}{-ik \sin(z + \beta_N)} \right] \quad (\text{A9})$$

which shows a pole singularity for  $z = \pm\beta_N$ , where  $2\beta_N$  is the angle subtended by the aperture at the distance  $\rho$  ( $2\beta_N \approx d/\rho$ ). This justifies the assumption made in Sec. III. We wish to note that for  $\rho \gg d$  (Fraunhofer approximation),  $\beta_N$  becomes negligible so that Eq. (A9) reproduces the well-known result (centric)  $\sin[k(d/2) \sin z]/k \sin z$ . In addition, as a test of this model, we have verified that the intensity of the field, as a function of  $z$  in the proximity of the aperture, has a shape in agreement with Eq. (A9) when complex values of  $\beta_N$  are considered; see Fig. 12.

- 
- [1] For a review on the subject see E.H. Hauge and J.A. Støvneng, *Rev. Mod. Phys.* **61**, 917 (1989).
- [2] F.E. Low and P.F. Mende, *Ann. Phys. (N.Y.)* **210**, 380 (1991).
- [3] Experiments with Josephson junctions have recently attracted the interest for the possibility of detecting macroscopic quantum tunneling. See D. Esteve, J. Martinis, C. Urbina, E. Turlot, M.H. Devoret, H. Grabert, and S. Linkwitz, *Phys. Scr.* **T29**, 121 (1989) for a carried out experiment; B.I. Ivlev and V.I. Melnikov, *Pis'ma Zh. Eksp. Teor. Fiz.* **41**, 116 (1985) [*Sov. Phys. JETP Lett.* **41**, 142 (1985)]; *Phys. Rev. Lett.* **55**, 1614 (1985) for an interesting proposal.
- [4] A. Ranfagni, D. Mugnai, P. Fabeni, and G.P. Pazzi, *Phys. Scr.* **42**, 508 (1990); *Appl. Phys. Lett.* **58**, 774 (1991); *Physica B* **175**, 283 (1991).
- [5] R.P. Feynman, R.B. Leighton, and M. Sands, *The Feynman Lectures on Physics* (Addison-Wesley, Reading, MA, 1977), Vol. 2, pp. 24–27.
- [6] Th. Martin and R. Landauer, *Phys. Rev. A* **45**, 2611 (1992). The electromagnetic experiments proposed in this article are partially realized by the microwave simulation reported in Ref. [4].
- [7] T.E. Hartman, *J. Appl. Phys.* **33**, 3427 (1962).
- [8] The results of Ref. [4] range in frequency between  $\sim 9.4$  and  $\sim 9.7$  GHz with a cutoff at  $\sim 9.5$  GHz.
- [9] A. Enders and G. Nimtz, *J. Phys. I (Paris)* **2**, 1693 (1992).
- [10] S. Bosanac, *Phys. Rev. A* **28**, 577 (1983).
- [11] D. Mugnai, A. Ranfagni, R. Ruggeri, and A. Agresti, *Phys. Rev. Lett.* **68**, 259 (1992).
- [12] This “anomaly” has been already considered in the literature, see C.R. Leavens and G.C. Aers, *Phys. Rev. B* **40**, 5387 (1989); H.A. Fertig, *Phys. Rev. Lett.* **65**, 2321 (1990).
- [13] T. Koryu Ishii and G.C. Giakos, *Microwaves and RF*, August 1991, p. 114.
- [14] F.E. Terman, *Electronic and Radio Engineering* (McGraw-Hill, New York, 1955), Chap. 5.
- [15] Even if this is not exactly true—that is, the signal velocity at  $\alpha = 0$  may be lower than  $c$ —from the obtained results a superluminal behavior clearly emerges at sufficiently large values of  $\alpha$ .
- [16] G. Toraldo di Francia, *Electromagnetic Waves* (Inter-

- science, New York, 1955), Chap. 10. See also (unpublished).
- [17] As for the meaning of the term “leaky wave,” see L.B. Felsen and N. Marcuvitz, *Radiation and Scattering of Waves* (Prentice-Hall, Englewood Cliffs, NJ, 1973), Secs. 5.3, 5.6, and 5.9. See also Chap. 4 for the general theory of the asymptotic evaluation of integrals.
- [18] This is not a surprising result when we consider that the leaky waves of Eq. (7) really propagate in the  $\beta_r$  direction with a velocity lower or at maximum (for  $\beta_i \rightarrow 0$ ) equal to  $c$ .
- [19] A. Ranfagni, D. Mugnai, and A. Agresti, *Phys. Lett. A* **158**, 161 (1991).
- [20] L. Brillouin, *Wave Propagation and Group Velocity* (Academic, New York, 1960).
- [21] G. Doetsch, *Theorie und Anwendung der Laplace Transformation* (Springer, Berlin, 1937).
- [22] S.K. Foong, *Phys. Rev. A* **46**, R707 (1992).
- [23] Yakir Aharonov and Lev Vaidman, *Phys. Rev. A* **41**, 11 (1990).
- [24] G. Toraldo di Francia, *La Diffrazione della Luce* (Einaudi, Torino, 1958).